Accepted Manuscript

Tanshinone IIa protects retinal endothelial cells against mitochondrial fission induced by methylglyoxal through glyoxalase I

Shuhong Qian, Yujin Qian, Dongxia Huo, Shijin Wang, Qingwen Qian

PII: S0014-2999(19)30370-X

DOI: https://doi.org/10.1016/j.ejphar.2019.172419

Article Number: 172419

Reference: EJP 172419

To appear in: *European Journal of Pharmacology*

Received Date: 1 January 2019

Revised Date: 24 May 2019

Accepted Date: 24 May 2019

Please cite this article as: Qian, S., Qian, Y., Huo, D., Wang, S., Qian, Q., Tanshinone IIa protects retinal endothelial cells against mitochondrial fission induced by methylglyoxal through glyoxalase I, *European Journal of Pharmacology* (2019), doi: https://doi.org/10.1016/j.ejphar.2019.172419.

This is a PDF file of an unedited manuscript that has been accepted for publication. As a service to our customers we are providing this early version of the manuscript. The manuscript will undergo copyediting, typesetting, and review of the resulting proof before it is published in its final form. Please note that during the production process errors may be discovered which could affect the content, and all legal disclaimers that apply to the journal pertain.

ACCEPTED MANUSCRIPT

1 **Tanshinone IIa protects retinal endothelial cells against mitochondrial fission induced by**
2 **methylglyoxal through glyoxalase I**

3 Shuhong Qian1, Yujin Qian2, Dongxia Huo3, Shijin Wang1, Qingwen Qian4,5*

4 1. Department of Clinical Laboratory, 1st Affiliated Hospital, Zhengzhou University, China

5 2 Australian Institute for Bioengineering and Nanotechnology, The University of Queensland,
6 Australia

7 3. College of Material Engineering, Zhengzhou University, China

8 4. Department of Internal Medicine, 1st Affiliated Hospital, Zhengzhou University, China

9 5. Department of Anatomy & Cell Biology, Iowa University, USA

10 *Corresponding Author

11 Qingwen Qian, 1st Affiliated Hospital, Department of Internal Medicine, Zhengzhou University,
12 No.40 Daxue Road, Zhengzhou, Henan 450052, China E-mail:qwqian@zzu.edu.cn

13

ACCEPTED MANUSCRIPT

14 **Abstract**

15 Advanced glycation end products (AGEs) play an important role in the onset of diabetic
16 retinopathy. Therefore, in the current study, we investigate whether and how Tanshinone IIa
17 (Tan IIa) from Salvia miltiorrhiza protects bovine retinal endothelial cells (BRECs) against
18 methylglyoxal (MGO) mediated cell dysfunction. The results showed that MGO reduced cell
19 viability in dose dependent manner. The treatment of Tan IIa (50 μM) significantly improved cell
20 viability induced by MGO in BRECs. MGO increased cellular reactive oxygen species formation
21 and cellular nitric oxide (NO) level; enhanced nox1 and iNOS mRNA levels; inhibited prdx1
22 mRNA level. The treatment of Tan IIa effectually ameliorated cellular oxidative stress. Exposure
23 of MGO resulted in mitochondrial fission and decrease of opa1 and mfn1. No significant
24 difference in mRNA levels of mfn2 and drp1 was detected between MGO and medium. Tan IIa
25 reduced mitochondrial fragmentation, enhanced the mRNA levels of mfn1 and opa1 in MGO
26 cultured BRECs. The short time exposure of cellular antioxidatants, dimethylthiourea (10mM)
27 and tiron (10mM) had no effect on mitochondrial fission although they ameliorated cellular
28 reactive oxygen species level. Moreover, overexpression of GLO1 increased key proteins of
29 mitochondrial fusion, including OPA1 and MFN1 in BRECs cultured with MGO. However,
30 inhibition of GLO1 by siRNA abolished the effect of Tan IIa on induction of mitochondrial fusion
31 in MGO cultured BRECs. In conclusion, MGO caused the injury of retinal endothelial cells
32 through induction of mitochondrial dysfunction and mitochondrial fission, the treatment of Tan
33 IIa ameliorated mitochondrial dysfunction and fission induced by AGEs through enhancing
34 GLO1.

35 **Keywords**: Taninone IIa, glycation, glyoxalase I, mitochondrial fission

36 **1. Introduction**

37 Retinopathy is one of major chronic micro-vascular complications in diabetes. Accumulation of
38 advance glycation end products (AGEs) play an important role in the development of diabetic
39 retinopathy (DR) (Feener and King, 1997). The initial formation of cellular AGEs is mainly from
40 non-enzymatic reaction of glucose and the reactive dicarbonyl metabolites of glucose, including
41 methylglyoxal (MGO) (Brownlee, 1995; Feener and King, 1997; Vlassara and Uribarri, 2014).
42 The increase of AGEs leads to up-regulate VEGF expression (Deissler et al., 2014), and
43 stimulates the secretion of pro-inflammatory cytokines (Nakamura et al., 2003), which increase
44 vascular permeability leaking and leukocyte aggregation in the retinal microvasculature (Otero
45 et al., 2001). Excessive MGO leads to accumulation of lipofuscin in RPE and inhibition of RPE
46 cell proliferation (Yoon et al., 2012). Plenty of evidences reveal that cellular oxidative stress and
47 mitochondrial dysfunction induced by AGEs trigger and deteriorate retinal dysfunction in
48 diabetes (Roy et al., 2017). In diabetic renal microvascular endothelial cells, mitochondrial
49 electron chain transporter complex III is impaired though the modification of arginine residues of
50 cytochrome C1 by MGO (Rosca et al., 2005). Besides that, oxidative stress increases
51 mitochondrial membrane permeability by opening mitochondrial inner membrane pores and
52 reducing membrane potential in diabetic cardiac myocytes (Van Remmen et al., 2001). In
53 pancreatic beta cells, exposure of glycated modification of bovine serum albumin (BSA) results
54 in the decrease of insulin secretin and defect of mitochondrial formation. Exposure of glycated-
55 BSA increases mitochondrial damage and Drp1 expression (Lo et al., 2015). Yu et al. have
56 reported that inhibition of AGEs receptor reduces mitochondrial fission in cardiomyocytes from
57 high fat diet induced obesity (Yu et al., 2017). However, the link between cellular oxidative
58 stress and mitochondrial dynamics induced by glycated modification in retinal endothelial cells is
59 unclear.

60 S. miltiorrhiza is widely used as a supplementary medicine in China, Korea and Japan. It has
61 been applied in the treatment of cardiovascular diseases and cerebrovascular diseases (Wang
62 et al., 2018). Tanshinones IIa (Tan IIa) is one of main lipophilic components from S. miltiorrhiza
63 (Gao et al., 2018). Tan IIa reduces VEGF secretion in human retinal pigment epithelial cells
64 (APRE19 cells) under hypoxic condition (Alzhrani et al., 2017). In human retinal endothelial cells,
65 Tan IIa inhibits VEGF and ICAM�1 mRNA levels in 25 mM glucose condition (Fan et al., 2017).
66 Tan IIa ameliorates mitochondrial membrane potential and mitochondrial permeability transition
67 in model of neuron and liver damage (Liu et al., 2010; Zhu et al., 2010). However, the
68 regulation of retinal mitochondrial fusion and fission by Tan IIa is not clear yet.

69 Therefore, in the current study, we explore whether Tan IIa protects retinal endothelial cell
70 against MGO mediated mitochondrial dysfunction and mitochondrial fission. We also investigate
71 the mechanism that mediates mitochondrial dynamics under cellular glycated modification
72 condition, particularly focus on the link between mitochondrial reactive oxygen species
73 formation and mitochondrial fission induced by MGO.

74

75

76

ACCEPTED MANUSCRIPT

77 **2. Materials and Methods**

78 2.1 Materials

79 Tanshinone IIa (chemical structure as Fig. 1) was purchased from National Institute for the
80 Control of Pharmaceutical and Biological Products, China. Collagenase IV, fibronectin, crystal
81 violet were from Sigma USA. CM-2',7'-dichlorodihydrofluorescein diacetate (H2DCFDA), 4-
82 Amino-5-Methylamino-2',7'-Difluorofluorescein Diacetate (DAF-FM), 5, 5′, 6, 6′-tetrachloro1, 1′, 3,
83 3′-tetraethyl-benzimidazolylcarbocyanine iodide (JC-1), Mitotracker red, Lipofectamine
84 RNAiMax® Transfection Reagent, Lipofectamine 2000 Transfection reagent, Opti-MEM 1
85 medium were from Life Technologies, USA. MGO was from Yuecheng Biotechnology, China.
86 GSH was from Kyowa, Japan. Trizol reagent was from Chengdu Yuqiang Technology Co. Ltd,
87 China. SYBR Green master mix was from MedChemExpress, China.

88 2.2 Cell culture

89 Bovine eyes were from local slaughtering house, the isolation and culture of retinal endothelial
90 cells was followed the protocol described by Caperandes A, et al (Capetandes and Gerritsen,
91 1990). Briefly, bovine retina was collected and homogenized. After collagenase IV digestion,
92 cells were seeded to fibronectin (Sigma)-coated dishes. Bovine retinal endothelial cells (BREC)
93 were used in current study after four or five passages.

94 2.3 Transient knockdown of glyoxalase I expression by RNAi

95 BREC cells were seeded into 6-well or 96-well plate. After reaching 80% confluence, cells were
96 transfected with GLOI or non-specific scrambled siRNAs using Lipofectamine RNAiMax®
97 according to the manufacturer's instructions in serum-free OptiMEM® media. After incubation
98 with transfection complexes for 6 h, the medium was changed to antibiotic-free media. The

99 double stranded siRNA sequences against bovine GLO RNAi were 5'' CAG GAA AUC AUG
100 UGA UUC AAG AUAT 3' and 5’ AUA UCU UGA AUC ACA UGA UUU CCU GUU 3'.

101 2.4 Transient overexpression of glyoxalase I expression

102 BREC cells were seeded into 6-well or 96-well plates. After reaching 80% confluence, cells
103 were transfected with GLOI vector and pcDNA3 using Lipofectamine 2000 according to the
104 manufacturer's instructions in serum-free OptiMEM® media. After incubation with transfection
105 complexes for 4.5 h, the medium was changed to complete growth media.

106 2.5 Cell viability using crystal violet assay

107 BREC cells were seeded in 96-well plates and treated with different conditions. Cells were fixed
108 with 4% formaldehyde solution and stained nuclei with 0.2% crystal violet solution. 1% SDS
109 solution was added to dissolve the staining particle, the absorbance of each well was obtained
110 at 570 nm.

111 2.6 Glyoxalase 1 activity and GSH level

112 The measurement of glyoxalase 1 activity was followed the protocol described by McLellan AC,
113 et al (McLellan and Thornalley, 1989). BREC cells were seeded to 6-well plates. Cellular lysate
114 was added to hemithioacetal, prepared by pre-incubating MGO and GSH. The standard assay
115 mixture contained 2 mm MGO and 2 mm GSH in a sodium phosphate buffer (100 mm, pH 6.6,
116 37 °C). GSH level was determined according to the manual described by commercial supplier,
117 Nanjing Jiancheng Bioengineering Institute.

118 2.7 Measurement of cellular reactive oxygen species and NO levels

ACCEPTED MANUSCRIPT

119 reactive oxygen species was determined using CM-H2DCFDA, and NO was measured by DAF-
120 FM. BREC cells were seeded to 96-well black plates with clear bottom. Cells were treated with
121 100 µM MGO with or without Tan IIa for 24 h. At the end of the experimental treatments, cells
122 were washed with PBS and loaded with probe, and incubated at 37°C for 10 min followed by a
123 PBS wash.

124 2.8 Measurement of mitochondrial membrane potential ($\Delta\psi_m$)

125 Mitochondrial membrane potential was measured by JC-1. JC-1, a cationic dye, exhibits
126 mitochondrial membrane potential-dependent aggregation detected as fluorescent aggregates
127 (red). Loss of mitochondrial membrane potential causes JC-1 to shift to monomeric for (green).
128 A decrease in red/green ratio is interpreted as a loss of mitochondrial membrane potential. After
129 treatment, BREC cells were incubated with JC-1 dye for 45 min at 37°C. The ratio of aggregate
130 (red) and monomer (green) is an indication of mitochondrial membrane potential.

131 2.9 Mitochondrial morphology

132 BREC cells were seeded in 96-well plates. Mitotracker red was used to stain mitochondria
133 following the described by manufacturer. Cells were treated with 100 µM MGO with/without
134 Tanshinone IIa for 24 h. Images were taken by confocal microscopy. All images were acquired
135 using a 40X oil immersion objective.

136 2.10 Realtime RT-PCR

137 BREC cells were seeded in 12-well plates. After the designed treatment, RNA was extracted by
138 Trizol. Quantity PCR was performed using the SYBR Green master mix. Primers: glo1 forward
139 primer: 5'-CGG CTT TGG AGG CTT GAG TA-3', reverse primer: 5'-AAC ACA AGC ACC ACT
140 TGC AC-3'; beta actin forward primer: 5'- CAG TCG GTT GGA TCG AGC AT-3' reverse primer:

ACCEPTED MANUSCRIPT

141 5’- TGG CTT TTG GGA AGG CAA AG-3’; inos forward primer: 5’-GGT GGA AGC AGT AAC
142 AAA GGA-3’, reverse primer: 5’-GAC CTG ATG TTG CCG TTG TTG-3’; prdx1 forward primer:
143 5’- TGG TGT CGG TCC TAT TTC AGT G-3’, reverse primer: 5’- GCT GTT GCT TTG AAC TGG
144 GG-3’; nox1 forward primer: 5’- CTC TGC TCG CTG CTT GAA TTT-3’ reverse primer: 5’- GTG
145 GAA GGC GAG GTT GTG AT-3’; drp1 forward primer: 5’-ACG AGT TAT GGA GGC GCT AA-
146 3’, reverse primer: 5’-AGC TCT TTC CAC TGC TCT GC-3’; mfn1 forward primer: 5’-TGC ACC
147 AAT GAA GTC AAC GC-3’, reverse primer: 5’-TGC AAG GAA CCA GTG TGT GT-3’; mfn2
148 forward primer: 5’-CAA GAG TCA GTA ACT CAG AAT TGG T-3’, reverse primer: 5’-GTC TGC
149 TGG TAC AAC TGG AAC-3’; opa1 forward primer: 5’-CCT TGC AAA ATT GGC ACC TGA-3’,
150 reverse primer: 5’-CCA GGT GAA CCT GTG GTG AA-3’;

151 2.11 Data Analysis and Statistics

152 The results were analyzed for statistical significance by GraphPad Prism software (GraphPad
153 Software) using ANOVA test with Tukey post hoc test or Mann-Whitney for comparisons
154 wherever appropriate. The results were shown as Mean ± S.E.M. and differences between
155 means were considered statistically significant when $p<0.05$.

156

157

ACCEPTED MANUSCRIPT

158 **3. Results**

159 3.1 Tan IIa rescued cell death induced by MGO in primary bovine retinal endothelial cells

160 The results showed that exposure with MGO led to a reduction of cell viability in dose
161 dependent manner (Fig. 2A). 10 μM MGO significantly decreased cell viability in comparison
162 with medium ($P<0.05$). The treatment of 50 μM Tan IIa, not 10 μM, significantly improved the
163 reduction of cell viability by MGO in BRECs ($P<0.01$, Fig. 2B). Furthermore, 50 μM Tan IIa
164 improved GLO1 activity and mRNA level in MGO cultured with BRECs (Fig. 2C and Fig. 2D). In
165 the meantime, Fig. 2E showed that the treatment of Tan IIa ameliorated the reduction of GSH in
166 MGO conditions ($P<0.01$). In summary, increase of general glycated modification by MGO
167 resulted in reduction of cell viability and inhibition of GLO1 mRNA, the treatment of Tan IIa
168 protected retinal endothelial cells against cellular impairs induced by MGO.

169 3.2 Tan IIa rescued cellular oxidative stress induced by MGO in primary bovine retinal
170 endothelial cells

171 It is known that oxidative stress plays a crucial role in endothelial dysfunction induced by MGO.
172 We monitored cellular oxidative stress level using fluorescent probe H2DCFDA. Results of Fig.
173 3A revealed that 100 μM MGO markedly enhanced cellular oxidative stress, compared with
174 vehicle ($P<0.005$). The treatment of Tan IIa ameliorated the induction of oxidative stress in
175 MGO ($P<0.005$). Furthermore, results of Fig. 3B and Fig. 3C showed that MGO caused the
176 significant reduction of prdx1 mRNA and increase of nox1 mRNA. The treatment of Tan IIa
177 significantly improved pdrx1 mRNA level ($P<0.01$), and reduced nox1 mRNA in MGO cultured
178 BRECs ($P<0.05$). Moreover, Fig. 3D and Fig. 3E displayed that MGO also stimulated cellular
179 nitic oxide (NO) level and iNOS mRNA level in comparison with vehicle. Tan IIa ameliorated
180 cellular NO level ($P<0.005$) and reduced iNOS mRNA ($P<0.001$), compared with MGO. In

181 conclusion, excessive MGO increased cellular oxidative stress, administration of Tan IIa
182 ameliorated oxidative stress through the increase of antioxidant enzyme and inhibition of
183 oxidative enzymes.

184 3.3 Tan IIa inhibited mitochondrial fission induced by MGO in primary bovine retinal endothelial
185 cells

186 Mitochondria are key cellular organelles of producing ATP. Electron gradient driven membrane
187 potential is crucial for ATP generation and mitochondrial dynamics. Reduction of mitochondrial
188 membrane potential results in low OPA1 level, therefore, leads to mitochondrial fission. Here,
189 we used JC-1 as the probe to detect mitochondrial membrane potential. Fig. 4A showed the
190 level of mitochondrial membrane potential decreased markedly after exposure with excessive
191 MGO. The treatment of Tan IIa increased significantly the level of mitochondrial membrane
192 potential in BREC cells with MGO ($P<0.05$).

193 MitoTracker Red was added to BREC cells to observe mitochondrial morphology using
194 fluorescent confocal microscopy. Fig. 4B and Fig. 4C showed MGO led to an increase of
195 mitochondrial fragmentation in comparison with medium. The treatment of Tan IIa reversed
196 mitochondrial fragmentation. The results of Fig. 4D, Fig. 4E, Fig. 4F and Fig. 4G displayed that
197 MGO reduced the expression of OPA1 and MFN1, the key proteins of mitochondrial fusion,
198 comparing with medium ($P<0.005$). The treatment of Tan IIa significantly restored the reduction
199 of OPA1 ($P<0.05$) and MFN1 ($P<0.005$) mRNA levels (Fig. 4C and Fig 4D). However, there was
200 no significant difference in mRNA level of MFN2 (one of the key protein of mitochondrial fusion)
201 and drp1 (the key protein of mitochondrial fission) among vehicle, MGO and MGO plus Tan IIa
202 treatment (Fig. 4E and 4F). In summary, the results revealed that the MGO inhibited OPA1 and
203 MFN1 mRNA levels and induced mitochondrial fission. The treatment of Tan IIa reduced
204 mitochondrial fission induced by accumulation of MGO in BRECs.

205 3.4 Short-term amelioration of cellular oxidative stress had no effect on mitochondrial fission
206 induced by MGO

207 The current results indicated that excessive cellular MGO led to increase of cellular oxidative
208 stress and mitochondrial fission. Therefore, in this section, we will explore whether cellular
209 oxidative stress contribute to mitochondrial fission induced by MGO. Fig. 5A showed that, 30
210 min treatment of dimethylthiourea (10mM) and tiron (10mM) significantly ameliorated cellular
211 reactive oxygen species level (P<0.005). However, 30 min treatment of dimethylthiourea and
212 tiron had no significant effect on OPA1, MFN1 and drp1 mRNA levels (Fig. 5B, Fig. 5C and Fig.
213 5D). In summary, the results revealed indirectly that the induction of mitochondrial fission by
214 MGO may be due to the glycated modification of key proteins involved in mitochondrial fusion
215 process.

216 3.5 Overexpression of glyoxalase I improved the mRNA levels of mitochondrial fusion related to
217 gene in MGO cultured BREC cells

218 According to the glycated prediction analysis from website
219 (http://www.cbs.dtu.dk/services/NetGlycate/), OPA1 and MFN1 have multiple glycated sites
220 (supplemental Fig.). We used western blot to test AGEs using commercial anti-methylglyoxal
221 antibody, no difference was detected between MGO and medium (data were not shown). The
222 reason may be due to that antibody has no cross reaction with bovine. As it is known that GLO1
223 is the key enzyme detoxifying reactive dicarbonyls (Jack and Wright, 2012). Therefore, in this
224 section, overexpression of GLO1 was used to reduce of protein glycated modification by MGO.
225 Results of Fig. 6A confirmed that overexpression of GLO1 increased GLO1 activity compared
226 with pcDNA (P<0.01). Data from Fig. 6B showed that overexpression of GLO1 improved cell
227 viability induced by MGO (P<0.05). Fig. 6C and Fig. 6D showed that overexpression of GLO1
228 increased the mRNA levels of MFN1 and OPA1. In summary, those results indirectly revealed

229 that the improvement of mitochondrial fission by overexpression of GLO1 is though reduction of
230 protein glycated modification.

231 3.6 Inhibition of GLO1 blocked the therapeutic effect of Tan IIa on MGO cultured BRECs

232 To explore whether the effect of Tan IIa is through GLO1, GLO1 expression was inhibited by
233 transiently transfected with GLO1 siRNA. The results of Fig. 7A confirmed that GLO1 mRNA
234 levels markedly inhibited after BRECs were transfected with GLO1 siRNA, compared with
235 scramble siRNA ($P<0.005$). Fig. 7B showed that inhibition of GLO1 expression by siRNA
236 deteriorated significantly cellular reactive oxygen species formation induced by MGO ($P<0.01$).
237 Furthermore, the treatment of Tan IIa did not ameliorate cellular reactive oxygen species
238 formation induced by MGO after inhibition of GLO1 expression. Fig. 7C and Fig. 7D further
239 demonstrated that the effect of Tan IIa on the induction of opa1 and mfn1 mRNA reduced after
240 inhibition of GLO1 by siRNA ($P<0.05$). In summary, all of those data revealed indirectly that the
241 effect of Tan IIa on amelioration of cellular reactive oxygen species formation and mitochondrial
242 fission was through GLO1.

243

ACCEPTED MANUSCRIPT

ACCEPTED MANUSCRIPT

244 **4. Discussion**

245 In current study, our results revealed that Tan IIa protected retinal endothelial cells against
246 mitochondrial fission induced by MGO through the improvement of protein glycated modification.
247 It is known that glycation is one of major causes of chronic microvascular endothelium
248 dysfunction, which shows increase of oxidative stress, endothelium leaking. The importance of
249 MGO on the development of vascular endothelium dysfunction has been explored extensively.
250 Exposure of MGO leads to loss of endothelial cells, basement membrane thickening, luminal
251 occlusion (Berlanga et al., 2005) and oxidative stress (Sena et al., 2012). Furthermore, in vitro
252 study mimicking hyperglycemia condition, overexpression of GLO1 ameliorates the impairment
253 of formation of tube-like structures, and reduces AGE formation in diabetic rats (Brouwers et al.,
254 2014). The mechanism that mediates glycation induced retinal endothelium dysfunction is not
255 fully clear yet. Our results demonstrated that excessive MGO reduced cell viability in dose
256 dependent manner in BRECs. 100 μM MGO increased cellular reactive oxygen species
257 formation and cytosol oxidative enzyme, NOX1 mRNA level; decreased cellular anti-oxidative
258 enzymes, prdx1 mRNA levels. Besides those, MGO also enhanced chronic inflammation and
259 impairs endothelial cell integrates (McVicar et al., 2015; Wang et al., 2014). Tan IIa has been
260 used in the treatment of cardiovascular disease and nephropathy (Li et al., 2018; Liang et al.,
261 2018; Yan et al., 2018). Tan IIa markedly inhibited diabetes induced proliferation, migration and
262 vascularization in human retinal endothelial cells (Fan et al., 2017), and inflammation in human
263 pigment endothelial cells (Lee et al., 2015). Chen X, et al. revealed that the treatment of Tan IIa
264 markedly improved diabetic nephropathy through enhancing SOD activity and reducing MDA
265 level (Chen et al., 2017). The results from BRECs confirmed that the treatment of 50 μM Tan IIa
266 rescued the reduction of cell viability, ameliorated the induction of general cellular oxidative
267 stress, inhibited NOX1 mRNA level and increased sirt1 and pdrx1 mRNA levels in BRECs
268 exposed with excess MGO.

269 Mitochondria is the key organelle of generating cellular oxidative stress. It is known that
270 mitochondria constantly produce reactive oxygen species during oxidative phosphorylation.
271 Endogenous protective system, such as unfolded proteins and anti-oxidative enzymes, can
272 maintain normal mitochondrial function (Baker et al., 2011; Nargund et al., 2012). However,
273 defective mitochondria may impair cellular function through generating excessive reactive
274 oxygen species formation and needs to be eliminated from mitochondrial network. Mitochondrial
275 inner fusion protein OPA1 is inactivated by inner membrane protease OMA1, which leads to
276 significant decrease of mitochondrial membrane potential (Ehses et al., 2009; Head et al., 2009).
277 In the meantime, the outer membrane fusion proteins, MFN1 and MFN2 are ubiquitinated.
278 Modified MFN1 and MFN2 are binding to p97 and then degraded by proteasomes (Tanaka et al.,
279 2010). When modified proteins were expended to the whole mitochondrial membrane,
280 mitochondrial fission is induced by activation of Drp1. Mid49, Mid51 and mitochondrial fission
281 factor are necessary for recruiting Drp1 to mitochondria membrane (Elgass et al., 2013).
282 Mitochondrial fission leads to lower mitochondrial membrane potential. Our results revealed that
283 100 μM MGO caused significant decrease of mitochondrial membrane potential, and increased
284 mitochondrial fragment and decreased MFN1 and OPA1 mRNA levels. The treatment of Tan IIa
285 inhibited mitochondrial fragment, enhanced the MFN1 and OPA1 mRNA level. In summary, the
286 treatment of Tan IIa can protect retinal endothelial cells against cellular oxidative stress and
287 mitochondrial fission induced by excessive MGO.

288 It is known that cellular excessive reactive oxygen species formation results in mitochondrial
289 fission, and increase of apoptosis (Wu et al., 2011; Youle and van der Bliek, 2012). Therefore,
290 in current study, we investigated whether mitochondrial fission induced by excessive MGO was
291 through cellular oxidative stress. Short term exposure of anti-oxidant (dimethylthiourea and tiron)
292 markedly ameliorated mitochondrial reactive oxygen species formation induced by MGO.
293 However, the treatment of dimethylthiourea and tiron did not alter mRNA levels of MFN1 and

294 OPA1. Those results suggest that general cellular glycated modification may play a crucial role
295 in the induction of mitochondrial fission in BRECs. According to bioinformatics analysis from
296 NetGlycate, both of OPA1 and MFN1 can be glycated modification (suppl Fig.). However, we
297 did not have direct evidence to confirm the bioinformatics analysis (data from western blot was
298 unable to detect the difference between control and MGO cultured BRECs. Images of western
299 blot did not show). The indirect experiment (GLO1 overexpression) was applied in this study. It
300 is well-known that GLO1 is the key enzyme to detoxify MGO (Xue et al., 2008). Imbalance of
301 MGO and GLO1 generates chronic vascular dysfunction, insulin resistance, ageing and
302 atherosclerosis (Navarrete Santos et al., 2017; Nigro et al., 2017; Petrie et al., 2018). Our
303 results demonstrated that overexpression of GLO1 increased GLO1 and rescued the reduction
304 of OPA1 and MFN1 mRNA by 100 μM MGO. Our results from GLO1 siRNA further revealed
305 that inhibition of GLO1 by siRNA markedly deteriorated mitochondrial reactive oxygen species
306 formation and mitochondrial fusion related proteins, including OPA1 and MFN1. The effect of
307 Tan IIa on amelioration of cellular reactive oxygen species formation and stimulation of opa1
308 and mfn1 mRNA was abolished after GLO1 expression was blocked by GLO1 siRNA.

309 In conclusion, the current study showed that the treatment of Tan IIa protected primary retinal
310 endothelial cells against cellular oxidative stress and reduction of mitochondrial fission. The
311 mechanism that mediated improvement of mitochondrial fission is though improvement of
312 general cellular glycated modification. The further investigation of therapeutic effect of Tan IIa
313 on diabetic retinopathy needs to explore in vivo research.

314 **Acknowledgments**

315 We thank Mr. Yuxuan Qian for refining the English language in this paper.

316 **Conflicts of Interest**

ACCEPTED MANUSCRIPT

ACCEPTED MANUSCRIPT

317 No potential conflicts of interest relevant to this article were reported.

318 **Reference**

319 Alzhrani, R.M., Alhadidi, Q., Bachu, R.D., Shah, Z., Dey, S., Boddu, S.H., 2017. Tanshinone IIA
320 Inhibits VEGF Secretion and HIF-1alpha Expression in Cultured Human Retinal Pigment
321 Epithelial Cells under Hypoxia. Current eye research 42, 1667-1673.
322 Baker, M.J., Tatsuta, T., Langer, T., 2011. Quality control of mitochondrial proteostasis. Cold
323 Spring Harb Perspect Biol 3.
324 Berlanga, J., Cibrian, D., Guillen, I., Freyre, F., Alba, J.S., Lopez-Saura, P., Merino, N., Aldama,
325 A., Quintela, A.M., Triana, M.E., Montequin, J.F., Ajamieh, H., Urquiza, D., Ahmed, N.,
326 Thornalley, P.J., 2005. Methylglyoxal administration induces diabetes-like microvascular
327 changes and perturbs the healing process of cutaneous wounds. Clin Sci (Lond) 109, 83-
328 95.
329 Brouwers, O., Niessen, P.M., Miyata, T., Ostergaard, J.A., Flyvbjerg, A., Peutz-Kootstra, C.J.,
330 Sieber, J., Mundel, P.H., Brownlee, M., Janssen, B.J., De Mey, J.G., Stehouwer, C.D.,
331 Schalkwijk, C.G., 2014. Glyoxalase-1 overexpression reduces endothelial dysfunction and
332 attenuates early renal impairment in a rat model of diabetes. Diabetologia 57, 224-235.
333 Brownlee, M., 1995. Advanced protein glycosylation in diabetes and aging. Annu Rev Med 46,
334 223-234.
335 Capetandes, A., Gerritsen, M.E., 1990. Simplified methods for consistent and selective culture
336 of bovine retinal endothelial cells and pericytes. Invest Ophthalmol Vis Sci 31, 1738-1744.
337 Chen, X., Wu, R., Kong, Y., Yang, Y., Gao, Y., Sun, D., Liu, Q., Dai, D., Lu, Z., Wang, N., Ge, S.,
338 Wang, F., 2017. Tanshinone IIA attenuates renal damage in STZ-induced diabetic rats via
339 inhibiting oxidative stress and inflammation. Oncotarget 8, 31915-31922.

ACCEPTED MANUSCRIPT

340 Deissler, H.L., Lang, G.K., Lang, G.E., 2014. Capacity of aflibercept to counteract VEGF-
341 stimulated abnormal behavior of retinal microvascular endothelial cells. Exp Eye Res 122,
342 20-31.
343 Ehses, S., Raschke, I., Mancuso, G., Bernacchia, A., Geimer, S., Tondera, D., Martinou, J.C.,
344 Westermann, B., Rugarli, E.I., Langer, T., 2009. Regulation of OPA1 processing and
345 mitochondrial fusion by m-AAA protease isoenzymes and OMA1. J Cell Biol 187, 1023-
346 1036.
347 Elgass, K., Pakay, J., Ryan, M.T., Palmer, C.S., 2013. Recent advances into the understanding
348 of mitochondrial fission. Biochim Biophys Acta 1833, 150-161.
349 Fan, K., Li, S., Liu, G., Yuan, H., Ma, L., Lu, P., 2017. Tanshinone IIA inhibits high
350 glucoseinduced proliferation, migration and vascularization of human retinal endothelial
351 cells. Mol Med Rep 16, 9023-9028.
352 Feener, E.P., King, G.L., 1997. Vascular dysfunction in diabetes mellitus. Lancet 350 Suppl 1,
353 SI9-13.
354 Gao, H., Huang, L., Ding, F., Yang, K., Feng, Y., Tang, H., Xu, Q.M., Feng, J., Yang, S., 2018.
355 Simultaneous purification of dihydrotanshinone, tanshinone I, cryptotanshinone, and
356 tanshinone IIA from Salvia miltiorrhiza and their anti-inflammatory activities investigation.
357 Sci Rep 8, 8460.
358 Head, B., Griparic, L., Amiri, M., Gandre-Babbe, S., van der Bliek, A.M., 2009. Inducible
359 proteolytic inactivation of OPA1 mediated by the OMA1 protease in mammalian cells. J
360 Cell Biol 187, 959-966.
361 Jack, M., Wright, D., 2012. Role of advanced glycation endproducts and glyoxalase I in diabetic
362 peripheral sensory neuropathy. Translational research : the journal of laboratory and
363 clinical medicine 159, 355-365.

364 Lee, I.T., Liu, S.W., Chi, P.L., Lin, C.C., Hsiao, L.D., Yang, C.M., 2015. TNF-alpha mediates
365 PKCdelta/JNK1/2/c-Jun-dependent monocyte adhesion via ICAM-1 induction in human
366 retinal pigment epithelial cells. PLoS One 10, e0117911.
367 Li, D., Wang, J., Sun, D., Gong, X., Jiang, H., Shu, J., Wang, Z., Long, Z., Chen, Y., Zhang, Z.,
368 Yuan, L., Guan, R., Liang, X., Li, Z., Yao, H., Zhong, N., Lu, W., 2018. Tanshinone IIA
369 sulfonate protects against cigarette smoke-induced COPD and down-regulation of CFTR
370 in mice. Sci Rep 8, 376.
371 Liang, R., Zhao, Q., Jian, G., Cheng, D., Wang, N., Zhang, G., Wang, F., 2018. Tanshinone IIA
372 Attenuates Contrast-Induced Nephropathy via Nrf2 Activation in Rats. Cell Physiol
373 Biochem 46, 2616-2623.
374 Liu, T., Jin, H., Sun, Q.R., Xu, J.H., Hu, H.T., 2010. The neuroprotective effects of tanshinone
375 IIA on beta-amyloid-induced toxicity in rat cortical neurons. Neuropharmacology 59, 595-
376 604.
377 Lo, M.C., Chen, M.H., Lee, W.S., Lu, C.I., Chang, C.R., Kao, S.H., Lee, H.M., 2015. Nepsilon-
378 (carboxymethyl) lysine-induced mitochondrial fission and mitophagy cause decreased
379 insulin secretion from beta-cells. Am J Physiol Endocrinol Metab 309, E829-839.
380 McLellan, A.C., Thornalley, P.J., 1989. Glyoxalase activity in human red blood cells fractioned
381 by age. Mech Ageing Dev 48, 63-71.
382 McVicar, C.M., Ward, M., Colhoun, L.M., Guduric-Fuchs, J., Bierhaus, A., Fleming, T.,
383 Schlotterer, A., Kolibabka, M., Hammes, H.P., Chen, M., Stitt, A.W., 2015. Role of the
384 receptor for advanced glycation endproducts (RAGE) in retinal vasodegenerative
385 pathology during diabetes in mice. Diabetologia 58, 1129-1137.
386 Nakamura, N., Hasegawa, G., Obayashi, H., Yamazaki, M., Ogata, M., Nakano, K., Yoshikawa,
387 T., Watanabe, A., Kinoshita, S., Fujinami, A., Ohta, M., Imamura, Y., Ikeda, T., 2003.
388 Increased concentration of pentosidine, an advanced glycation end product, and

ACCEPTED MANUSCRIPT

389 interleukin-6 in the vitreous of patients with proliferative diabetic retinopathy. Diabetes Res
390 Clin Pract 61, 93-101.
391 Nargund, A.M., Pellegrino, M.W., Fiorese, C.J., Baker, B.M., Haynes, C.M., 2012. Mitochondrial
392 import efficiency of ATFS-1 regulates mitochondrial UPR activation. Science 337, 587-590.
393 Navarrete Santos, A., Jacobs, K., Simm, A., Glaubitz, N., Horstkorte, R., Hofmann, B., 2017.
394 Dicarbonyls induce senescence of human vascular endothelial cells. Mech Ageing Dev
395 166, 24-32.
396 Nigro, C., Leone, A., Raciti, G.A., Longo, M., Mirra, P., Formisano, P., Beguinot, F., Miele, C.,
397 2017. Methylglyoxal-Glyoxalase 1 Balance: The Root of Vascular Damage. Int J Mol Sci
398 18.
399 Otero, K., Martinez, F., Beltran, A., Gonzalez, D., Herrera, B., Quintero, G., Delgado, R., Rojas,
400 A., 2001. Albumin-derived advanced glycation end-products trigger the disruption of the
401 vascular endothelial cadherin complex in cultured human and murine endothelial cells.
402 Biochem J 359, 567-574.
403 Petrie, J.R., Guzik, T.J., Touyz, R.M., 2018. Diabetes, Hypertension, and Cardiovascular
404 Disease: Clinical Insights and Vascular Mechanisms. Can J Cardiol 34, 575-584.
405 Rosca, M.G., Mustata, T.G., Kinter, M.T., Ozdemir, A.M., Kern, T.S., Szweda, L.I., Brownlee, M.,
406 Monnier, V.M., Weiss, M.F., 2005. Glycation of mitochondrial proteins from diabetic rat
407 kidney is associated with excess superoxide formation. Am J Physiol Renal Physiol 289,
408 F420-430.
409 Roy, S., Kern, T.S., Song, B., Stuebe, C., 2017. Mechanistic Insights into Pathological Changes
410 in the Diabetic Retina: Implications for Targeting Diabetic Retinopathy. Am J Pathol 187,
411 9-19.
412 Sena, C.M., Matafome, P., Crisostomo, J., Rodrigues, L., Fernandes, R., Pereira, P., Seica,
413 R.M., 2012. Methylglyoxal promotes oxidative stress and endothelial dysfunction.
414 Pharmacol Res 65, 497-506.

415 Tanaka, A., Cleland, M.M., Xu, S., Narendra, D.P., Suen, D.F., Karbowski, M., Youle, R.J., 2010.
416 Proteasome and p97 mediate mitophagy and degradation of mitofusins induced by Parkin.
417 J Cell Biol 191, 1367-1380.
418 Van Remmen, H., Williams, M.D., Guo, Z., Estlack, L., Yang, H., Carlson, E.J., Epstein, C.J.,
419 Huang, T.T., Richardson, A., 2001. Knockout mice heterozygous for Sod2 show
420 alterations in cardiac mitochondrial function and apoptosis. Am J Physiol Heart Circ
421 Physiol 281, H1422-1432.
422 Vlassara, H., Uribarri, J., 2014. Advanced glycation end products (AGE) and diabetes: cause,
423 effect, or both? Curr Diab Rep 14, 453.
424 Wang, H., Wei, T., Wang, X., Zhang, L., Yang, M., Chen, L., Song, W., Wang, C., Chen, C.,
425 2018. Transcriptome Analyses from Mutant Salvia miltiorrhiza Reveals Important Roles for
426 SmGASA4 during Plant Development. Int J Mol Sci 19.
427 Wang, J., Lin, J., Schlotterer, A., Wu, L., Fleming, T., Busch, S., Dietrich, N., Hammes, H.P.,
428 2014. CD74 indicates microglial activation in experimental diabetic retinopathy and
429 exogenous methylglyoxal mimics the response in normoglycemic retina. Acta Diabetol 51,
430 813-821.
431 Wu, S., Zhou, F., Zhang, Z., Xing, D., 2011. Mitochondrial oxidative stress causes mitochondrial
432 fragmentation via differential modulation of mitochondrial fission-fusion proteins. FEBS J
433 278, 941-954.
434 Xue, M., Qian, Q., Adaikalakoteswari, A., Rabbani, N., Babaei-Jadidi, R., Thornalley, P.J., 2008.
435 Activation of NF-E2-related factor-2 reverses biochemical dysfunction of endothelial cells
436 induced by hyperglycemia linked to vascular disease. Diabetes 57, 2809-2817.
437 Yan, S.H., Zhao, N.W., Geng, Z.R., Shen, J.Y., Liu, F.M., Yan, D., Zhou, J., Nie, C., Huang,
438 C.C., Fang, Z.Y., 2018. Modulations of Keap1-Nrf2 signaling axis by TIIA ameliorated the
439 oxidative stress-induced myocardial apoptosis. Free Radic Biol Med 115, 191-201.

ACCEPTED MANUSCRIPT

ACCEPTED MANUSCRIPT

440 Yoon, K.D., Yamamoto, K., Ueda, K., Zhou, J., Sparrow, J.R., 2012. A novel source of
441 methylglyoxal and glyoxal in retina: implications for age-related macular degeneration.
442 PLoS One 7, e41309.
443 Youle, R.J., van der Bliek, A.M., 2012. Mitochondrial fission, fusion, and stress. Science 337,
444 1062-1065.
445 Yu, Y., Wang, L., Delguste, F., Durand, A., Guilbaud, A., Rousselin, C., Schmidt, A.M., Tessier,
446 F., Boulanger, E., Neviere, R., 2017. Advanced glycation end products receptor RAGE
447 controls myocardial dysfunction and oxidative stress in high-fat fed mice by sustaining
448 mitochondrial dynamics and autophagy-lysosome pathway. Free Radic Biol Med 112, 397-
449 410.
450 Zhu, B., Zhai, Q., Yu, B., 2010. Tanshinone IIA protects rat primary hepatocytes against carbon
451 tetrachloride toxicity via inhibiting mitochondria permeability transition. Pharm Biol 48, 484-
452 487.
453
454
455

456 **Figure Legends**

457 **Figure 1. Chemical structure of Tan IIa**

458 **Figure 2. Tan IIa rescued cellular death led by cellular glycation.** a. Cell viability was
459 determined by crystal violet assay after exposure with MGO for 24 h. MGO reduced cell viability
460 in dose dependent manner. * P<0.05, **P<0.01 and *** P<0.005 compared with medium. b.
461 Crystal violet assay showed the protective effect of Tan IIa. 10 and 50 μM Tan IIa increased cell
462 viability under the condition of 100 μM MGO. ** P<0.01 compared with 100 μM MGO. c. GLO1
463 activity was determined in BRECs. Experimental conditions were: medium, 100 μM MGO, 50
464 μM Tan IIa and 100 μM MGO plus 50 μM Tan IIa for 24 h. # P<0.05 compared with 100 μM
465 MGO. d. GLO1 mRNA level decreased after exposure with MGO for 24 h. The treatment of 50
466 μM improved GLO1 mRNA level, *P<0.05, compared with MGO. e. GSH level was monitored in
467 BRECs under different experimental conditions. **P<0.01 indicates significant difference
468 compared with MGO.

469 **Figure 3. The treatment of Tan IIa ameliorated oxidative stress induced by cellular**
470 **glycated modification.** a. Cellular reactive oxygen species formation was measured by
471 fluorescent probe, CM-H2DCFDA. *** P<0.005 compared with medium. ### P<0.005 compared
472 with MGO. b. prdx1 c. nox1 mRNA levels were determined using Bio-Rad SYBR green
473 supermix kit. **P<0.01 indicates significant difference compared with medium, and ## P<0.01
474 indicates statistical significance compared with MGO. d. Cellular NO level was measured by
475 DAF-FM. *** P<0.005 compared with medium. ### P<0.005 compared with MGO. e. iNOS
476 mRNA levels were determined using Bio-Rad SYBR green supermix kit. *** P<0.005 indicates
477 significant difference compared with medium, and ## P<0.01 indicates statistical significance
478 compared with MGO.

ACCEPTED MANUSCRIPT

479 **Figure 4. Tan IIa rescued mitochondrial fission induced by MGO.** a. JC-1 was used to
480 measure mitochondrial membrane potential. The experiments repeated 3 times. Data are
481 shown as means ± S.E.M.. *** $P<0.005$ indicates statistically significant difference relative to
482 medium, and # $P<0.05$ indicates statistical significance related to 100 μM MGO. b.
483 Representative confocal images (63X) of mitochondrial morphology in BRECs. Mitochondria
484 were stained by mitotracker red. c. Cells with fragmented mitochondria were counted under a
485 confocal microscope. *** $P<0.005$ compared with medium; ## $P<0.01$ compared with 100 μM
486 MGO. d. OPA1 e. MFN1 f. MFN2 and g. Drp1 mRNA levels were determined by realtime RT-
487 PCR. *** $P<0.005$ indicates statistically significant difference relative to medium, and # $P<0.05$,
488 ## $P<0.01$ indicates statistical significance related to 100 μM MGO.

489 **Figure 5. Short-term amelioration of cellular oxidative stress had no effect on**
490 **mitochondrial fission induced by MGO in BRECs.** a. cellular reactive oxygen species
491 formation was evaluated as described above. Data are shown as means ± S.E.M. as
492 determined. *** $P<0.005$ indicates statistically significant difference relative to medium. ###
493 $P<0.005$ indicates statistically significant difference relative to 100 μM MGO. b. OPA1 c. MFN1
494 and d. Drp1 mRNA levels were determined by realtime RT-PCR. *** $P<0.005$ indicates
495 statistically significant difference relative to medium.

496 **Figure 6. Overexpression of GLO1 enhanced mitochondrial fusion key proteins'**
497 **expression.** a. GLO1 activity was determined, the detail method was described in Materials and
498 Methods. ** $P<0.01$ indicates statistically significant difference relative to transfection with
499 pcDNA. ## $P<0.01$ indicates statistically significant difference related to MGO cultured BRECs,
500 which were transfected with pcDNA. b. Cell viability was determined by crystal violet assay. ***
501 $P<0.005$ indicates statistically difference related to BRECs transfected with pcDNA. # $P<0.05$
502 indicates statistically difference related to MGO cultured BRECs transfected with pcDNA. c.
503 OPA1 and d. MFN1 mRNA levels were determined by realtime RT-PCR. ***$P<0.005$ indicates

504 statistically significant difference relative to BRECs transfected with pcDNA. # $P<0.05$ indicates
505 statistically difference related to MGO cultured BRECs transfected with pcDNA.

506 **Figure 7. Inhibition of GLO1 by siRNA abolished the effect of Tan IIa on cellular reactive**
507 **oxygen species formation and mitochondrial fusion proteins expression.** a. GLO1 mRNA
508 levels were determined by realtime RT-PCR. ** $P<0.01$, ***$P<0.005$ indicates statistically
509 significant difference relative to scramble siRNA. # $P<0.05$, ### $P<0.005$ indicates statistically
510 significant difference relative to 100 μM MGO treated BRECs transfected with scramble siRNA.
511 $ $P<0.05$ indicates statistically significant difference relative to 100 μM MGO and 50 μM Tan IIa
512 treated BRECs transfected with scramble siRNA. b. Cellular reactive oxygen species level was
513 determined by CM-H2DCFDA. **$P<0.01$, *** $P<0.005$ indicates statistically difference related to
514 MGO and scramble siRNA, ## $P<0.01$ indicates statistically significant difference relative to
515 MGO treated BRECs transfected with scramble siRNA. $ $P<0.05$ indicates statistically
516 significant difference relative to 100 μM MGO and 50 μM Tan IIa treated BRECs transfected
517 with scramble siRNA. c. OPA1 and d. MFN1 mRNA levels were determined by realtime RT-
518 PCR. ** $P<0.01$ indicates statistically significant difference relative to scramble siRNA. ##
519 $P<0.01$ indicates statistically significant difference relative to 100 μM MGO treated BRECs
520 transfected with scramble siRNA. $ $P<0.05$ indicates statistically significant difference relative to
521 100 μM MGO and 50 μM Tan IIa treated BRECs transfected with scramble siRNA.

522

523 **Supplemental figure**

524 **Figure Glycated site prediction in OPA1 and MFN1.** Potential glycated sites in A. OPA1 B.
525 MFN1 was analyzed using http://www.cbs.dtu.dk/services/NetGlycate/. Screenshot of analysis
526 indicated OPA1 and MFN1 might be glycated.

ACCEPTED MANUSCRIPT

527

ACCEPTED MANUSCRIPT

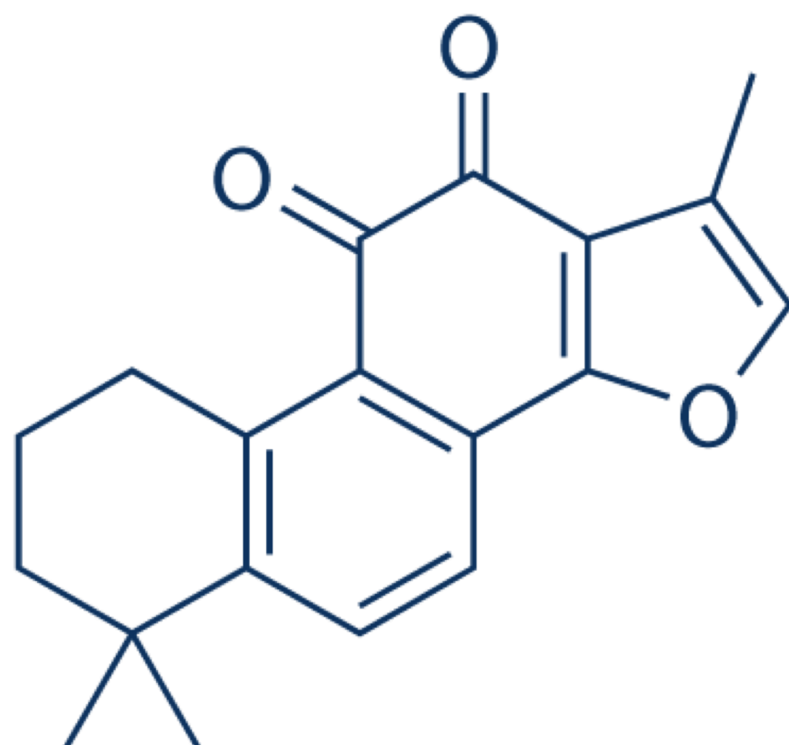
O
O
O

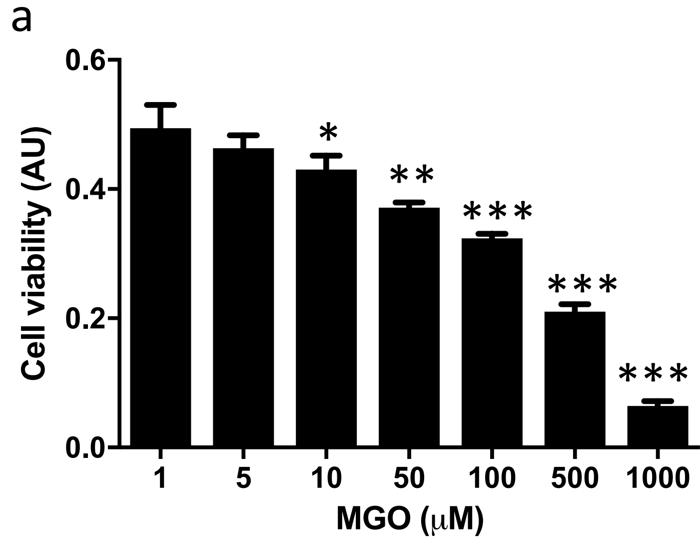
a
Cell viability (AU)
0.6
0.4
0.2
0.0
*
**
***
***
***
1
5
10
50
100
500
1000
MGO (μM)

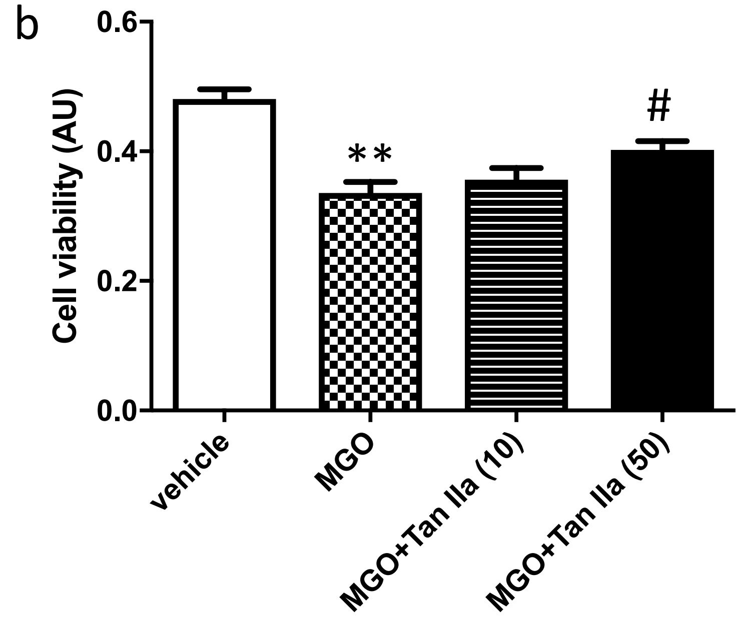
b
Cell viability (AU)
0.6
0.4
0.2
0.0
**
#
vehicle
MGO
MGO+Tan IIa (10)
MGO+Tan IIa (50)

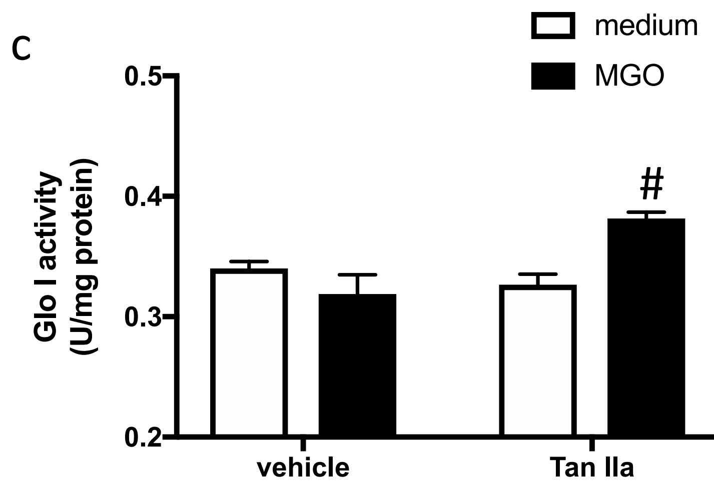
c
medium
MGO
Glo I activity
(U/mg protein)
0.5
0.4
0.3
0.2
#
vehicle
Tan IIa

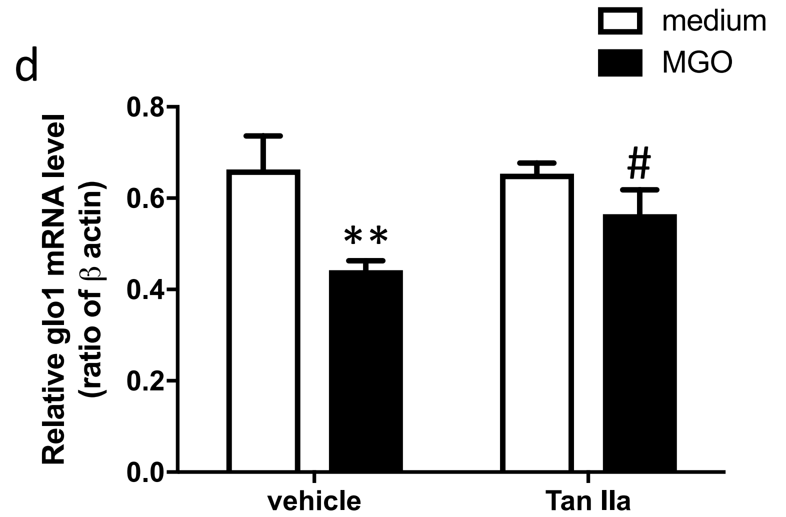
d
medium
MGO
Relative glo1 mRNA level
(ratio of β actin)
0.8
0.6
0.4
0.2
0.0
**
#
vehicle
Tan IIa

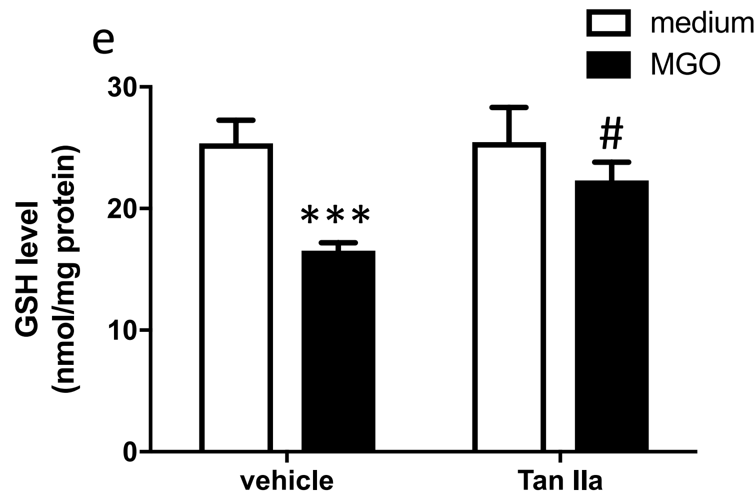
e
medium
MGO
GSH level
(nmol/mg protein)
30
20
10
0
***
#
vehicle
Tan IIa

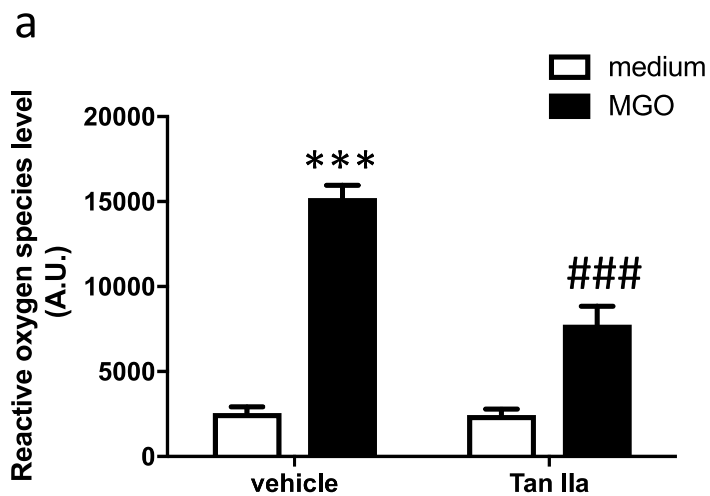
a
medium
MGO
Reactive oxygen species level
(A.U.)
20000
15000
10000
5000
0
***
###
vehicle
Tan IIa

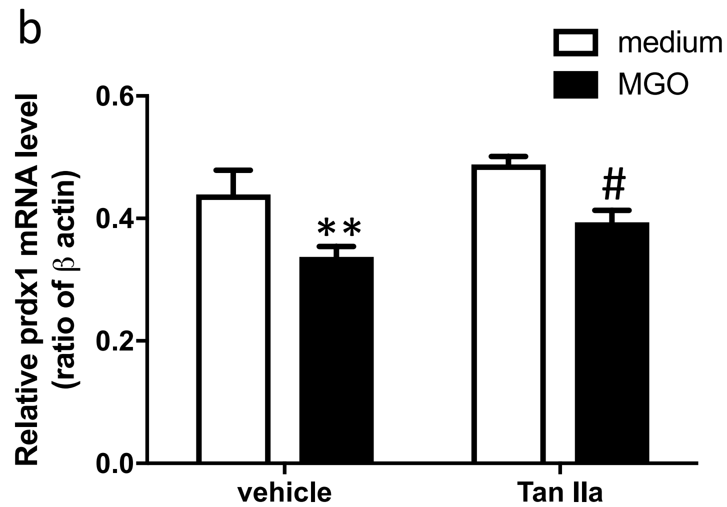
b
medium
MGO
Relative prdx1 mRNA level
(ratio of β actin)
0.6
0.4
0.2
0.0
**
#
vehicle
Tan IIa

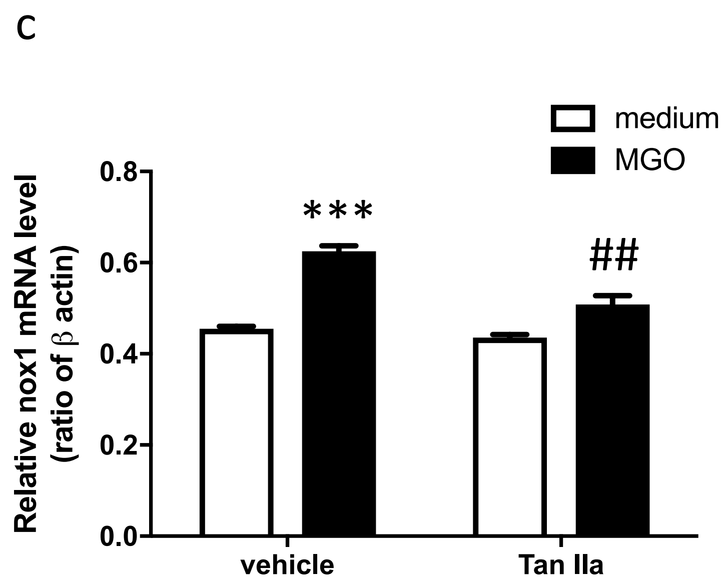
c
medium
MGO
Relative nox1 mRNA level
(ratio of β actin)
0.8
0.6
0.4
0.2
0.0
***
##
vehicle
Tan IIa

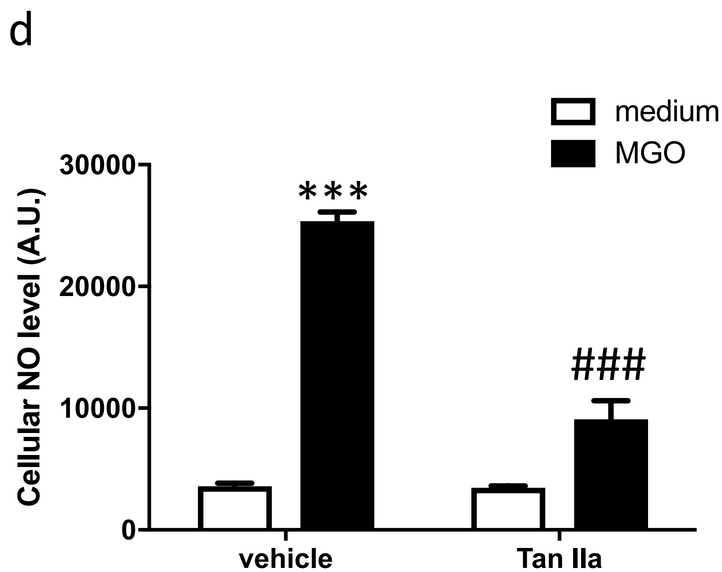
d
medium
MGO
Cellular NO level (A.U.)
30000
20000
10000
0
***
###
vehicle
Tan IIa

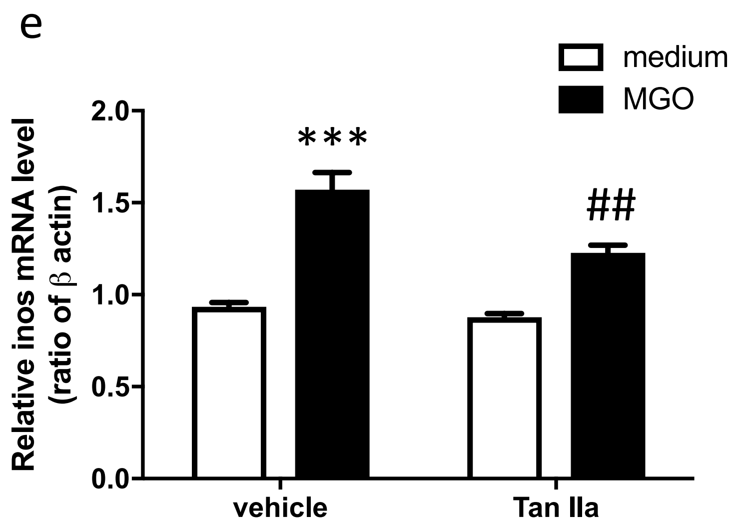
e
medium
MGO
Relative inos mRNA level
(ratio of β actin)
2.0
1.5
1.0
0.5
0.0
***
##
vehicle
Tan IIa

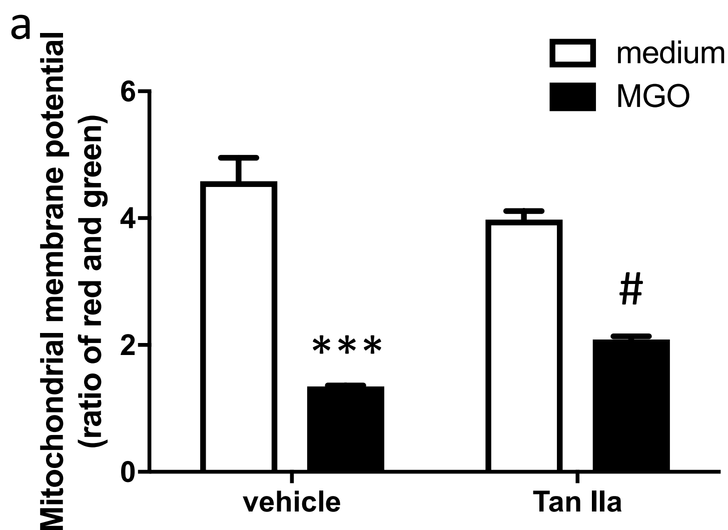
a
medium
MGO
Mitochondrial membrane potential (ratio of red and green)
6
4
2
0
***
#
vehicle
Tan IIa

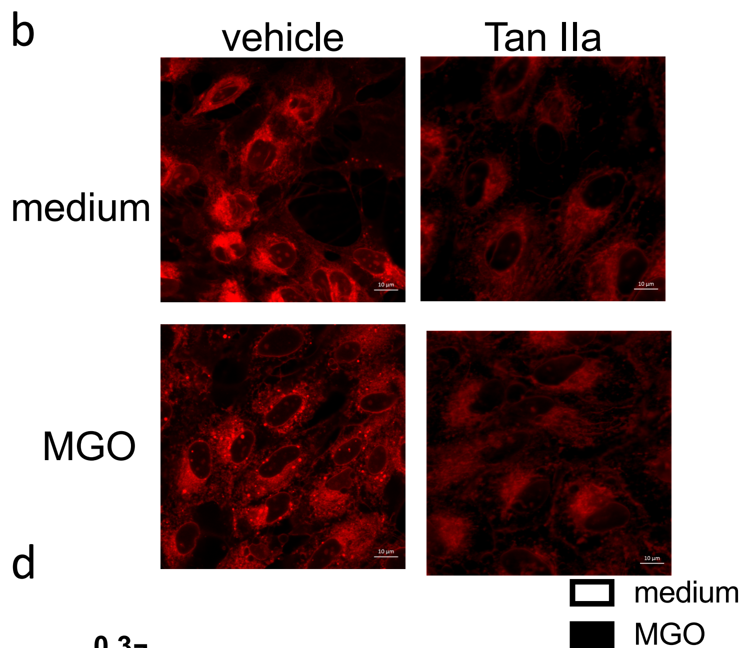
b
vehicle
Tan IIa
medium
MGO

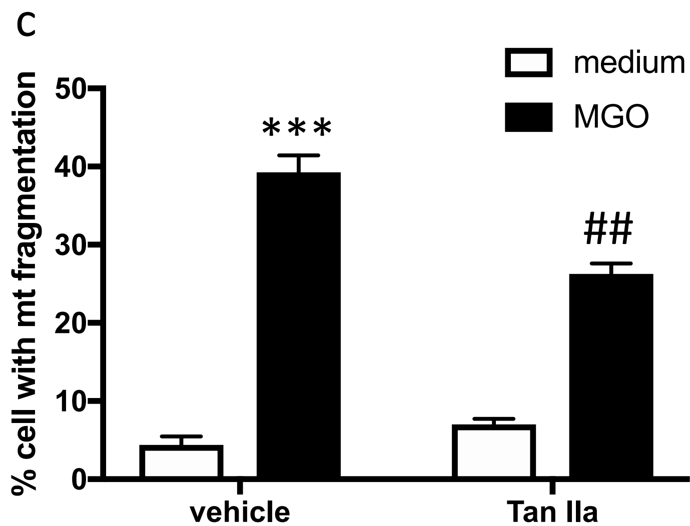
c
medium
MGO
% cell with mt fragmentation
50
40
30
20
10
0
***
##
vehicle
Tan IIa

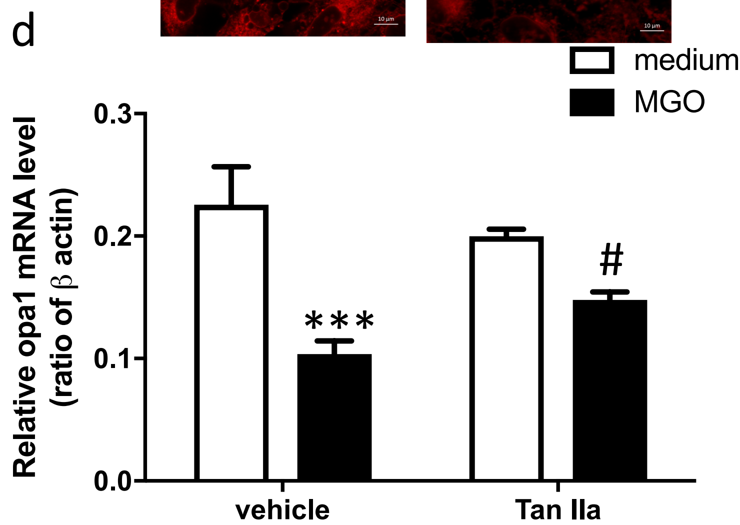
d
medium
MGO
Relative opa1 mRNA level (ratio of β actin)
0.3
0.2
0.1
0.0
***
#
vehicle
Tan IIa

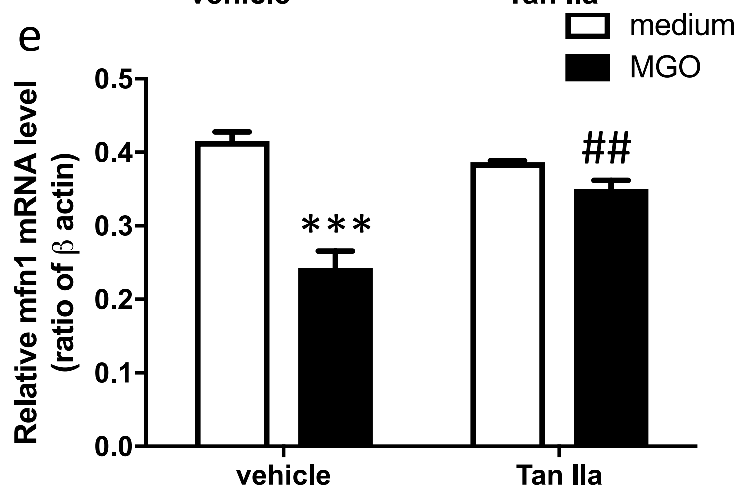
e
medium
MGO
Relative mfn1 mRNA level (ratio of β actin)
0.5
0.4
0.3
0.2
0.1
0.0
***
##
vehicle
Tan IIa

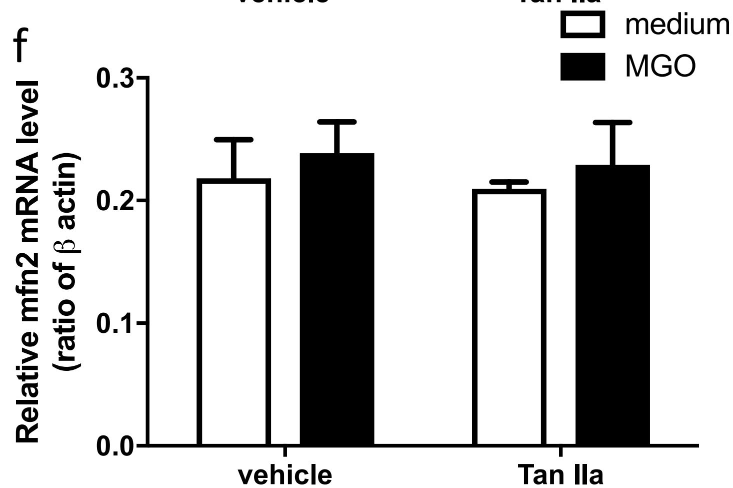
f
medium
MGO
Relative mfn2 mRNA level (ratio of β actin)
0.3
0.2
0.1
0.0
vehicle
Tan IIa

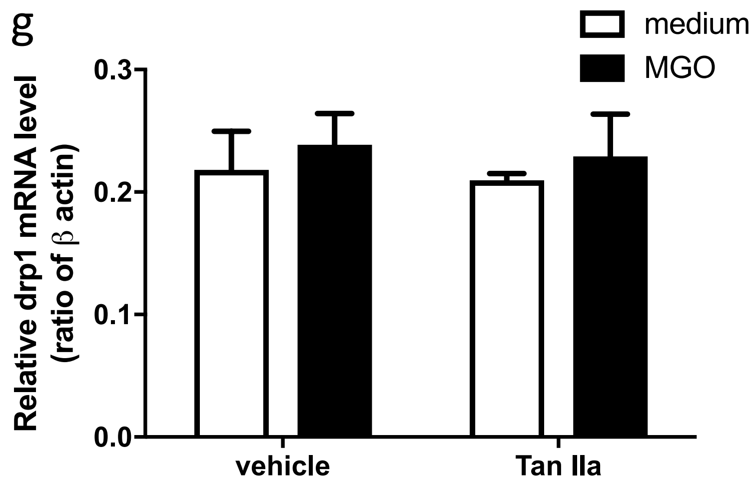
g
medium
MGO
Relative drp1 mRNA level (ratio of β actin)
0.3
0.2
0.1
0.0
vehicle
Tan IIa

a

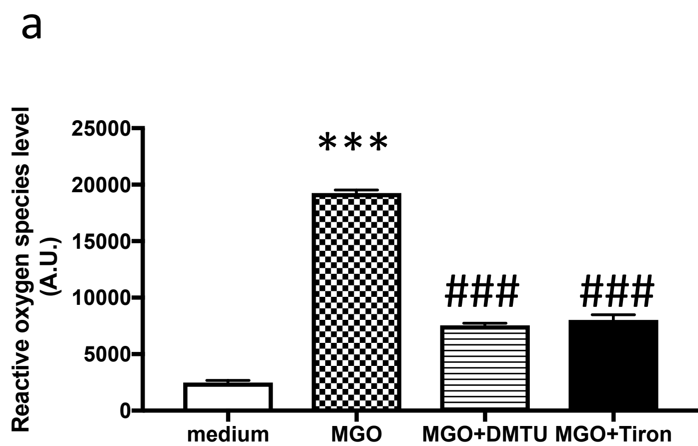

b

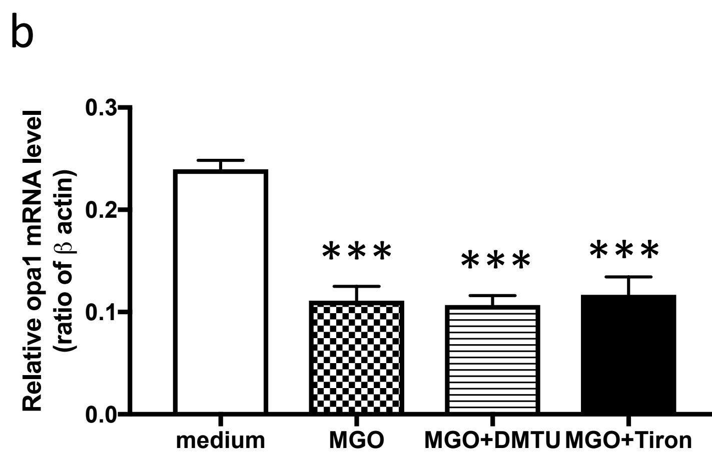

c

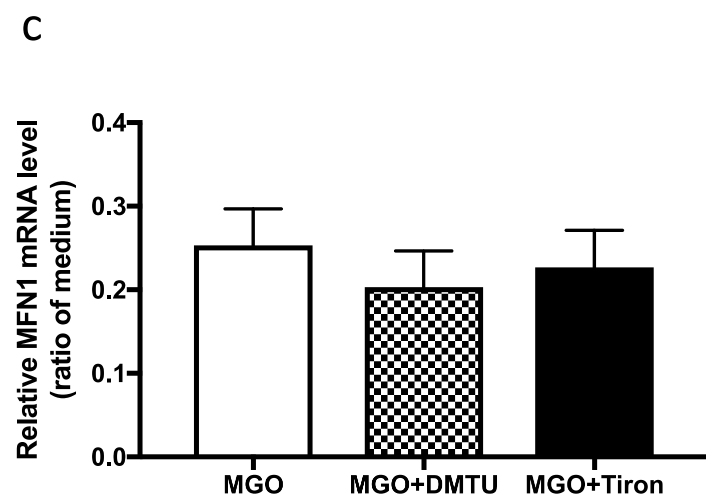

d

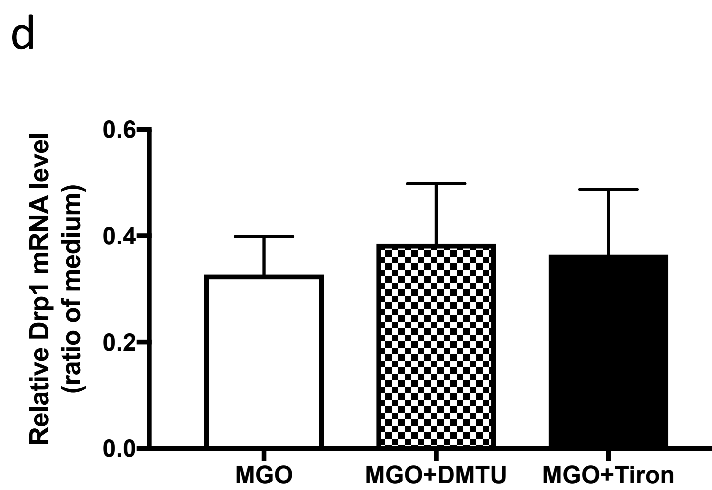

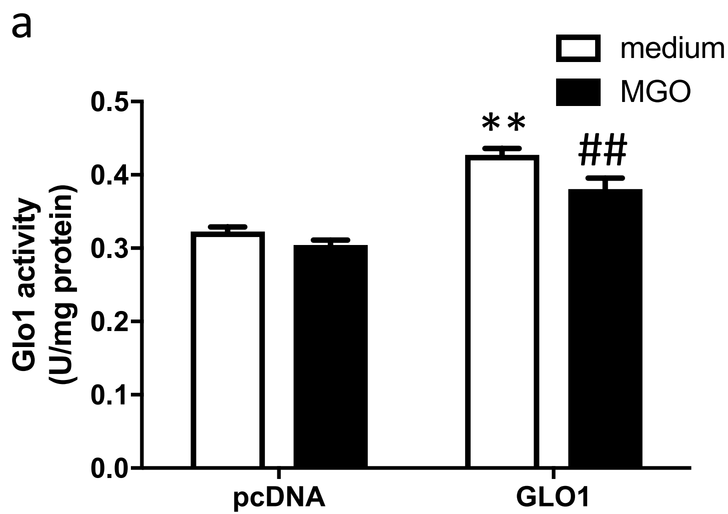
a
medium
MGO
Glo1 activity
(U/mg protein)
0.0
0.1
0.2
0.3
0.4
0.5
**
##
pcDNA
GLO1

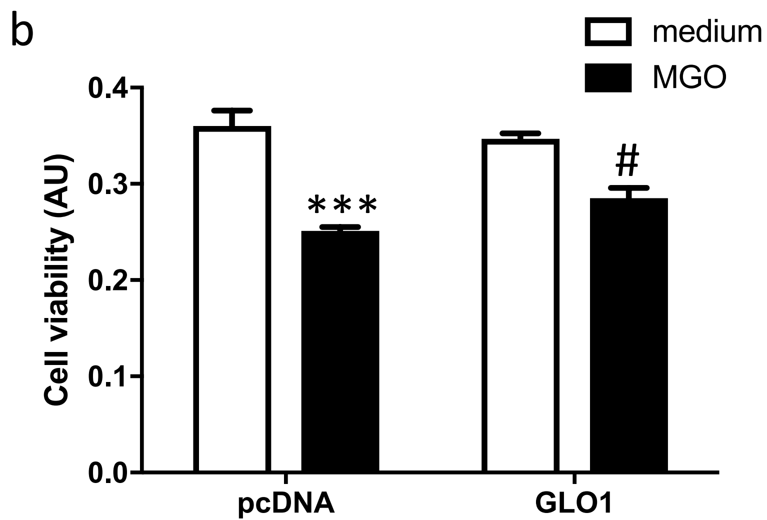
b
medium
MGO
Cell viability (AU)
0.0
0.1
0.2
0.3
0.4
***
#
pcDNA
GLO1

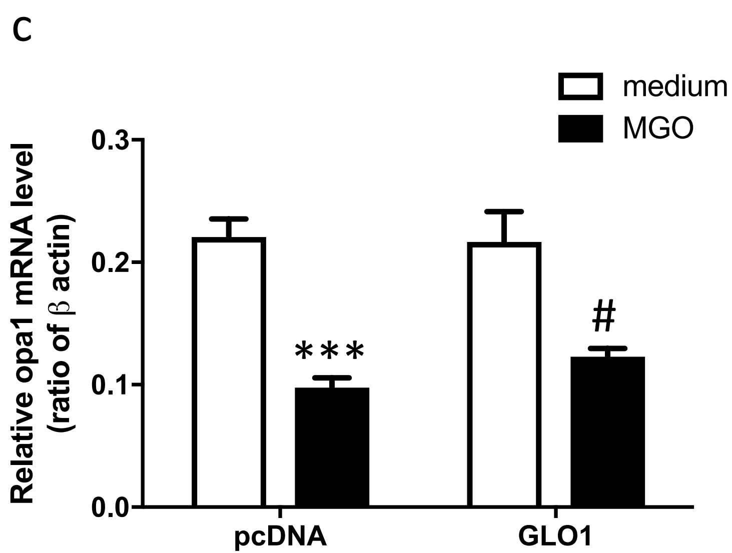
c
medium
MGO
Relative opa1 mRNA level
(ratio of β actin)
0.0
0.1
0.2
0.3
***
#
pcDNA
GLO1

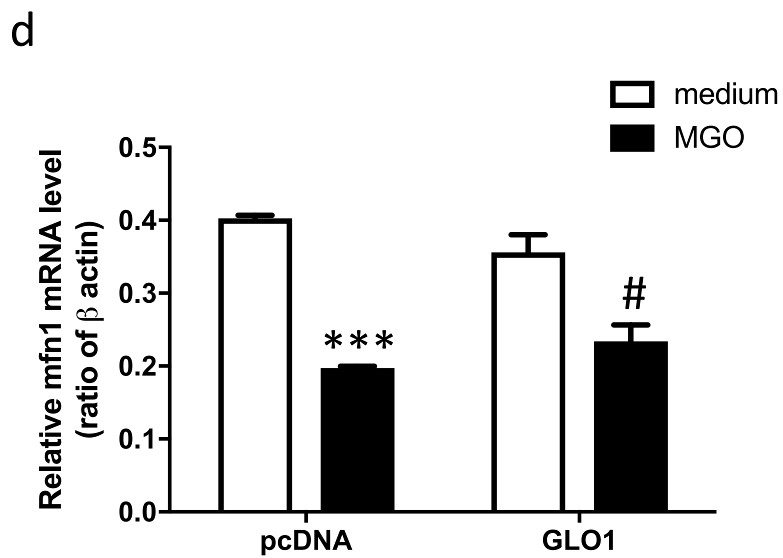
d
medium
MGO
Relative mfn1 mRNA level
(ratio of β actin)
0.0
0.1
0.2
0.3
0.4
0.5
***
#
pcDNA
GLO1

a

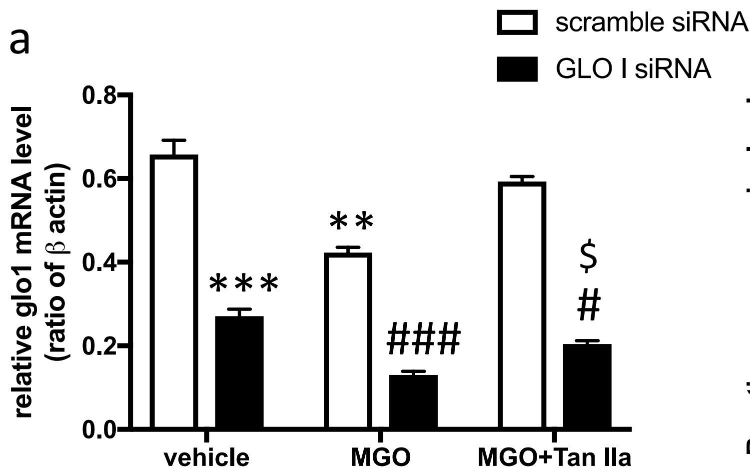

b

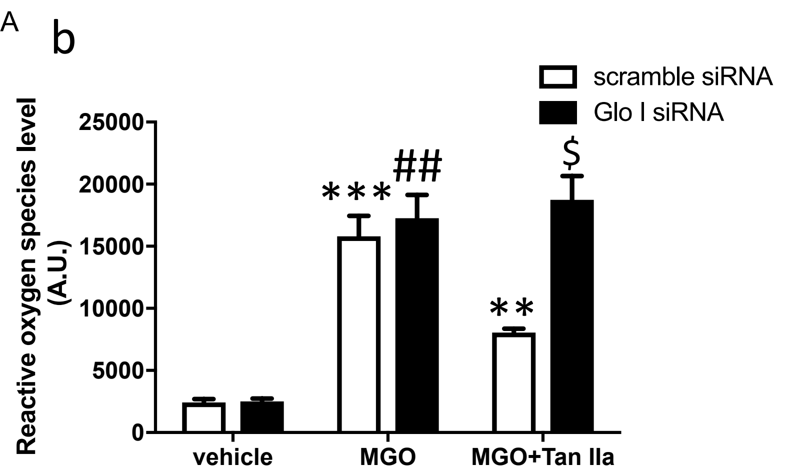

c

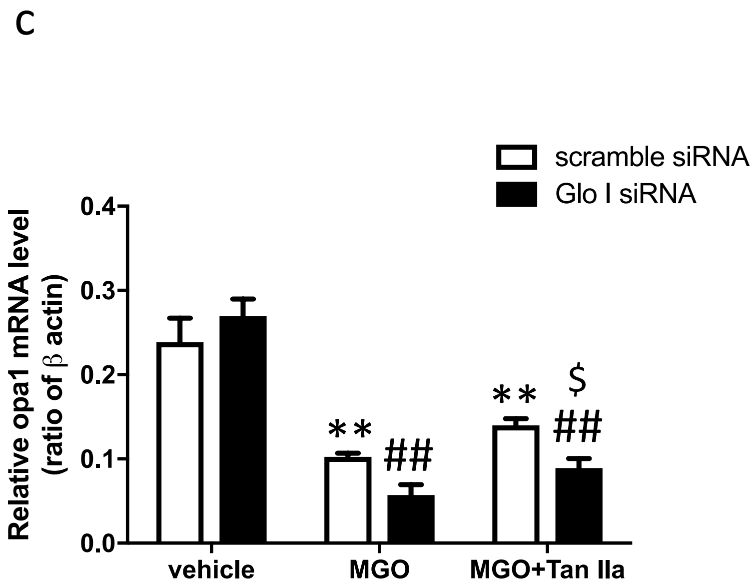

d